Published in Geochimica et Cosmochimica Acta 157, 198-212, 2015
which should be used for any reference to this work

Carbon and chlorine isotopologue fractionation of chlorinated hydrocarbons during diffusion in water and low permeability sediments

Philipp Wanner *, Daniel Hunkeler

Centre for Hydrogeology & Geothermics (CHYN), University of Neuchâtel, Rue Emil Argand 11, CH-2000 Neuchâtel, Switzerland

Abstract

To identify reactive processes in diffusion dominated water-saturated systems using compound-specific isotope analysis (CSIA), the effect of the diffusive transport process on isotope ratios needs to be known. This study aims to quantify the magnitude of carbon and chlorine isotopologue fractionation of two chlorinated hydrocarbons (trichloroethene (TCE) and 1,2-dichloroethane (1,2-DCA)) during diffusion in the aqueous phase and to relate for the first time laboratory with field results. Diffusion coefficient ratios in the aqueous phase were experimentally quantified with a modified Stokes diffusion cell. The experiment revealed a significant shift of carbon and chlorine isotopologue ratios of TCE and 1,2-DCA during diffusion. For both TCE and 1,2-DCA, the magnitude of the shift of chlorine isotopologue ratios was larger (TCE: $D_{132}/D_{130} = 0.99963 \pm 0.00003$; 1,2-DCA: $D_{102}/D_{100} = 0.99939 \pm 0.00003$) in comparison to carbon isotopologue ratios (TCE: $D_{131}/D_{130} = 0.99978 \pm 0.00006$; 1,2-DCA: $D_{101}/D_{100} = 0.99977 \pm 0.00004$), which is consistent with the larger mass difference between stable chlorine compared to carbon isotopes. Determined diffusion coefficients for carbon and chlorine isotopologues of TCE and 1,2-DCA follow an inverse power law form ($D \propto m^{-\beta}$) with $\beta < 0.5$ revealing that the magnitude of isotopologue fractionation of TCE and 1,2-DCA is lower than in the previously postulated kinetic theory ($D \propto m^{-0.5}$). To relate laboratory with field results, a water-saturated clay core from a VOC contaminated site was retrieved and subsampled as a function of depth to assess possible shifts in isotopologue ratios during downward diffusion of VOCs into the low permeable clay. Observed small shifts of TCE carbon and chlorine isotopologue ratio profiles were consistent with laboratory determined diffusion coefficient ratios, demonstrated by a 1D-diffusion model. Further 1D-simulations for shorter diffusion periods (5–10 years) than observed in the retrieved clay core (45 years), revealed a larger effect on TCE chlorine and carbon isotopologue ratio profiles. Thus, the diffusive transport process in water-saturated low permeability sediments only impairs the identification of reactive processes using compound-specific isotope analysis (CSIA) during short diffusion periods and for reactive processes with small enrichment factors.

1. INTRODUCTION

Due to industrial activities, groundwater contamination by chlorinated hydrocarbons is a widespread problem (Pankow and Cherry, 1996). When chlorinated hydrocarbons are released as dense non-aqueous phase liquid (DNAPL), vertical transportation through the unsaturated zone into aquifer systems usually occurs due to high density and low viscosity of DNAPLs (Cotel et al., 2011). During the further migration in aquifer systems, DNAPLs tend to accumulate on top of low permeability zones and diffuse into them (Feenstra et al., 1991; Johnson and Pankow,

* Corresponding author. Tel.: +41 32 718 26 22.
E-mail address: philipp.wanner@unine.ch (P. Wanner).

1992; Parker et al., 2004; Falta, 2005; Seyedabbasi et al., 2012). In these zones, frequently more reducing conditions are encountered and (bio)degradation of chlorinated hydrocarbons possibly occurs (Damgaard et al., 2013).

Compound-specific stable isotope analysis (CSIA) has been developed to track such (bio)chemical transformation processes and to relate contaminant sources to down gradient contamination. This method is generally based on the assumption, that only bond cleavage of organic molecules (i.e. (bio)chemical transformation processes) is associated with isotope effects (Hunkeler et al., 1999; Lollar et al., 2001; Meckenstock et al., 2004; Elsner et al., 2005; Hunkeler et al., 2005; Hunkeler et al., 2011). However, recent studies have shown that physical processes also can fractionate isotopes such as gas diffusion (Bouchard et al., 2008a,b), vaporization and air water partitioning (Harrington et al., 1999; Huang et al., 1999; Poulson and Drever, 1999; Kuder et al., 2009; Shin and Lee, 2010; Hunkeler et al., 2011; Jeannottat and Hunkeler, 2013), which potentially complicates the identification of (bio)chemical transformation processes using CSIA. In contrast to these processes, the effect of diffusion in the aqueous phase and water-saturated low permeability materials on isotope ratios has received little attention so far. In particular, isotope fractionation during diffusion could impair the identification of reactive processes in diffusion dominated saturated low permeability sediments using CSIA. Consequently, the quantification of a potential isotopic effect during diffusion of chlorinated hydrocarbons is indispensable to track reactive processes in diffusion dominated low permeability sediments such as clays.

Most previous studies in groundwater hydrology assumed that isotope fractionation of dissolved ions and noble gases during diffusion in the aqueous phase follows either the hydrodynamic theory (Berkowitz and Wan, 1987; Biswas and Bagchi, 1997; Chong and Hirata, 1998; McManus et al., 2002; Chernyavsky and Wortmann, 2007) or alternatively the kinetic theory, which was developed for gaseous mixtures (Senftle and Bracken, 1954; Desaulniers et al., 1985; Clark and Fritz, 1997; Peeters et al., 2003; Appelo and Postma, 2005; Donahue et al., 2008; LaBolle et al., 2008). The hydrodynamic theory assumes that a solute molecule moves through a continuum solvent with a specified viscosity and the diffusion coefficient is commonly described by the well-known Stokes–Einstein relation (Cussler, 2009):

$$D = \frac{k_B T}{6\pi\mu R_0} \tag{1}$$

where D (m^2/s) is the diffusion coefficient, k_B (J/K) is Boltzmann's constant, T (K) is the temperature, μ (kg/ms) refers to the viscosity of the solvent and R_0 (m) is the solute radius.

In the framework of the Stokes–Einstein relation, the diffusion coefficient of a dissolved species is radius but not mass dependent. Therefore, the hydrodynamic theory foresees no fractionation between isotopically distinct species differing in one or more neutrons, since an additional neutron increases the mass significantly but not necessarily the radius of the dissolved species. In contrary, in the framework of the kinetic theory, the diffusion coefficient of a dissolved species is mass dependent and the ratio between two diffusion coefficients of two isotopically distinct species is proportional to the inverse square root of their reduced masses:

$$\frac{D_H}{D_L} = \left(\frac{\mu_L}{\mu_H}\right)^{0.5} \tag{2}$$

where D_H (m^2/s) is the diffusion coefficient of the heavy isotope, D_L (m^2/s) is the diffusion coefficient of the light isotope and μ_L and μ_H refer to the reduced masses ($\mu_i = m_i M_i / m_i + M_i$) of the diffusing species, where m_i and M_i are solute and solvent masses.

For diffusing gases Eq. (2) can be simplified by assuming that the mass of the molecules of the medium (M_i) is infinitively large in comparison to the diffusing molecules ($M_i \gg m_i$) (Ballentine et al., 2002; Lippmann et al., 2003; Peeters et al., 2003; Strassmann et al., 2005; Zhou et al., 2005; Richter et al., 2006; Klump et al., 2007; Bourg and Sposito, 2008). Therefore, the reduced mass in Eq. (2) becomes to $\mu_i \rightarrow m_i$ since $m_i + M_i \rightarrow M_i$. This simplification leads to the kinetic "square root" relation:

$$\frac{D_H}{D_L} = \left(\frac{m_L}{m_H}\right)^{0.5} \tag{3}$$

where m_L and m_H refer to the molecular weights of the diffusing species.

Although the kinetic theory (Eq. (3)) was commonly used for estimating the magnitude of isotope fractionation during diffusion in the aqueous phase, it has been long known that this theory is not suitable, especially in liquid water, when a hydrodynamic behavior becomes more important (Alder et al., 1974; Nuevo et al., 1995). Recent studies emphasized this incorrect assumption by showing experimentally that the kinetic square root relation (Eq. (3)) overestimates the magnitude of isotope fractionation during diffusion in liquid water. Several studies (Richter et al., 2006; Eggenkamp and Coleman, 2009; Tempest and Emerson, 2013) demonstrated that the exponent in Eq. (3) ranges between 0 and 0.2 for diffusing ions (Li^+, Na^+, K^+, Mg^{2+}, Cl^-, Br^-) and noble gases (Ar, Ne) and that a more general power law model with an exponent $\beta < 0.5$ is more suitable to quantify isotope fractionation due to aqueous phase diffusion:

$$\frac{D_H}{D_L} = \left(\frac{m_L}{m_H}\right)^{\beta} \tag{4}$$

Molecular dynamic simulations (Bourg and Sposito, 2007, 2008; Bourg et al., 2010) confirmed the validity of the general power law model (Eq. (4)) for quantifying isotope fractionation during diffusion in liquid water. Bourg and Sposito (2007) revealed an inverse proportionality between beta values and the residence time of nearest water molecules surrounding dissolved ions (Li^+, Cl^-, Mg^{2+}). Moreover, by expanding molecular dynamic simulations to noble gases (Ar, Ne) and metal cations (Na^+, K^+, Cs^+, Ca^{2+}), Bourg and Sposito (2008) and Bourg et al. (2010) confirmed the generality of the inverse power law (Eq. (4)) for a wider range of solutes. Due to the wider

spectra of assessed species, Bourg et al. (2010) demonstrated, that the value of β (Eq. (4)) also depends, in addition to the residence time of nearest water molecules, on solute radius and valence state. Thus, diffusive transport process in the aqueous phase can be considered as an intermediate between a hydrodynamic and a kinetic behavior. Furthermore, Lavastre et al. (2005), Bourg and Sposito (2008), Beekmann et al. (2011) showed, that a general inverse power law form (Eq. (4)) is also valid at the field scale for assessing diffusive isotope fractionation of chlorine ($^{37}Cl/^{35}Cl$) and noble gases ($^{40}Ar/^{36}Ar$, $^{22}Ne/^{20}Ne$) in diffusion dominated saturated low permeable clays.

In contrast to ions, chlorinated hydrocarbons are dissolved as uncharged molecules in water. A given chlorinated hydrocarbon exists as species with different weight, denoted as isotopologues, as the elements (C, Cl, H) constituting the molecule have several stable isotopes. Compared to ions, less information is available in the literature regarding isotopologue fractionation during diffusive transport of organic compounds in water. Some studies used deuterated vs. non-deuterated compounds to determine isotopologue fractionation in ambient liquid water at the laboratory scale, as they are easy to measure. However, the results are conflicting, since some studies obtained beta values close to the kinetic theory (e.g. 0.455 for toluene and ethylbenzene isotopologue pairs) (Jin et al., 2014), while other studies received lower beta values close to the values obtained for diffusing ions (e.g. 0.063 for isopropanol (IPA) and 0.023 for tertiary butyl alcohol (TBA)) (LaBolle et al., 2008). This raises the question of the representativeness of the approach for natural abundance studies. In contrast, a few studies evaluated isotopologue fractionation of organic compounds at natural abundance under controlled laboratory conditions by addressing one type of isotopologue: Zhang and Krooss (2001) and Schloemer and Krooss (2004) assessed carbon isotopologue fractionation of methane and ethane, while Jin et al. (2014) assessed chlorine isotopologue fractionation of cis-1,2-dichloroethene (cDCE) and trichloroethene (TCE). These studies received beta values close to those for diffusing ions and clearly lower than 0.5, postulated in the kinetic theory (methane and ethane: 0.021–0.055, cDCE: 0.088 and TCE: 0.043). Furthermore, studies addressing isotopologue fractionation in saturated systems at the field scale are limited to modelling studies assuming a kinetic beta value of 0.5 (LaBolle et al., 2008; Rolle et al., 2010; Van Breukelen and Rolle, 2012). Thus, a study relating laboratory measured beta with measured field values and addressing more than one type of isotopologue pair of a specific organic compound (e.g. C and Cl types) is lacking.

In this study, diffusion coefficient ratios were for the first time determined for isotopes with distinct mass differences (C and Cl) within the same molecule and related to isotopologue ratio profiles at a field site, where transport is likely diffusion dominated. At the laboratory scale, diffusion coefficient ratios of carbon and chlorine isotopologue pairs of two common chlorinated organic groundwater contaminants, 1,2-dichloroethane (1,2-DCA) and TCE, were determined using a modified Stokes diffusion cell. At the field scale, a water-saturated clay core was retrieved from the bottom of a contaminated site and subsampled as a function of depth to evaluate possible shifts of TCE carbon and chlorine isotopologue ratios during downward diffusion into the clay. To compare field and laboratory data, field isotopologue ratio profiles were simulated using a 1D-diffusion model based on the laboratory determined diffusion coefficient ratios. The new insight into isotopologue fractionation of chlorinated hydrocarbons during diffusion in the aqueous phase provides a basis for identifying reactive processes in diffusion dominated low permeability sediments using CSIA.

2. EXPERIMENTAL DESIGN OF MODIFIED STOKES' DIFFUSION CELL

We used a modified Stokes' diffusion cell to quantify isotopologue fractionation during aqueous phase diffusion. Stokes' diffusion cell design (Stokes, 1950) is a well-accepted and commonly used method to determine diffusion coefficients of dissolved species in aqueous solutions (Vangeet and Adamson, 1964; Mills et al., 1968; Lo, 1974; Wedlake and Dullie, 1974; Asfour, 1983; Asfour and Dullien, 1983; Cussler, 2009). The concept relies on a horizontal separation of two well stirred compartments by a frit with small pore sizes (diameter: 5–7 μm). The lower compartment contains a dissolved species, while the upper compartment is filled with pure water. Because of the concentration gradient between the two compartments and the small pore size of the frit, the dissolved species in the lower compartment is exclusively transported by diffusion through the frit into the upper compartment. Diffusion coefficients are determined using the concentration difference between the two compartments, diffusion time and the previously determined diffusion cell constant. The latter is derived from species with known diffusion coefficients and is a correction factor for tortuosity and porosity effects affecting the diffusing species in the frit (Vangeet and Adamson, 1964; Mills et al., 1968; Lo, 1974; Wedlake and Dullie, 1974; Asfour, 1983; Asfour and Dullien, 1983; Cussler, 2009).

For the present study, the classical Stokes' diffusion cell design was modified to determine diffusion coefficient ratios for carbon and chlorine isotopologue pairs differing in one heavy isotope in ambient liquid water at constant temperature (22 °C). The intention of the modification was to maintain a maximal concentration gradient between the two compartments over time, by keeping the concentration in the upper compartment close to zero. This provides the advantage, that a constant rate of isotopologue accumulation was achieved in the lower compartment, which corresponds to a typical Rayleigh type behavior. The prevention of an equilibration between the source and the sink compartment is also an improvement in comparison to earlier diffusion experiments (Richter et al., 2006). In the earlier experiments, diffusion occurs from a small source container into a large sink container ($V_{sink}/V_{source} \sim 300$), during which equilibration occurred at the latest stage of the experiment between the source and the sink container. The modification was implemented by continuously renewing the water in upper compartment. For this purpose,

deionized water was passed at a rate of 10 ml/min through the upper compartment, by connecting it to a clean water reservoir placed higher than the diffusion cell (see Fig. 1 for details). The lower compartment was filled with an aqueous solution, containing either TCE or 1,2-DCA. The solutions of the two compartments of the modified diffusion cell were stirred with the help of a magnetic plate set vertically on the side of the cell, to stir the magnetic bars inside the two compartments (Fig. 1). This prevented the formation of boundary layers above and below the porous frit and ensured a homogenous concentration in the two compartments of the modified diffusion cell. To produce more data, two diffusion cells (named P2 and P3) were used simultaneously. The lower compartment of the used diffusion cells had volumes of 41.0 mL (P3) and 40.9 mL (P2), respectively and the upper compartments volumes of 34.0 mL (P3) and 35.0 mL (P2), respectively. The porous frit of both cells has the same pore size (1.0–1.6 μm diameter; data from manufacturer). Experiments of different duration were performed and samples were taken at the beginning and the end of each experiment from the lower compartment.

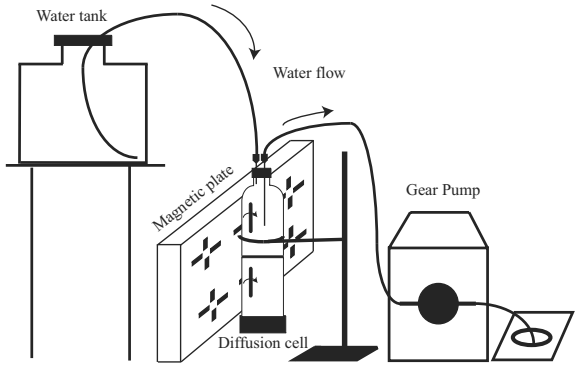

Fig. 1. Set up of modified Stokes' diffusion cell experiment.

The governing equation for diffusive transport within the modified diffusion cells can be expressed according to Fick's law of diffusion:

$$V_{\text{lower}} \frac{dC_{\text{lower}}}{dt} = -Aj \tag{5}$$

where V_{lower} (L) is the volume of the lower compartment, $\frac{dC_{\text{lower}}}{dt}$ (mg/L/s) corresponds to the temporal change in concentration, A is the area of the frit (m^2) and j (mg/m^2s) is the diffusive flux.

Within the frit a linear concentration gradient was assumed (quasi-steady-state), which has been proven as a reasonable assumption (Mills et al., 1968; Wedlake and Dullie, 1974). Thus, the diffusive flux across the porous frit is defined as follows according to the given geometric conditions of the diffusion cells:

$$j = \frac{D_e(C_{\text{lower}} - C_{\text{upper}})}{L} \tag{6}$$

with

$$D_e = D_0 \phi \tau \tag{7}$$

where D_0 (m^2/s) is the diffusion coefficient in free solution, ϕ (-) is the porosity, τ (-) is the tortuosity factor, L (m) refers to the thickness of the frit, D_e (m^2/s) is the effective diffusion coefficient and C_{lower} (mg/L) and C_{upper} (mg/L) are the concentrations in the lower and upper compartment, respectively.

The tortuosity factor in Eq. (7) includes the lowering of the diffusive transport rate due to the curved diffusion paths in the porous media in comparison to the straight paths in free solutions. Commonly tortuosity factors are expressed as the squared ratio between the length of the diffusion path in porous media and the diffusion path in free solution (Bear, 1972; Steefel and Maher, 2009):

$$\tau = \left(\frac{L}{L_E}\right)^2 \tag{8}$$

where L (m) is the diffusion path length in a free solution and L_E (m) is the diffusion path length in porous media.

Due to the continuous renewal of the water, the concentration in the upper compartment of the diffusion cell is close to zero. Inserting Eqs. (6) and (7) with $C_{\text{upper}} = 0$ in Eq. (5) leads to:

$$V_{\text{lower}} \frac{dC_{\text{lower}}}{dt} = -\frac{D_0 \phi \tau A C_{\text{lower}}}{L} \tag{9}$$

Rearranging and integrating formula 9 under the given boundary conditions, leads to the concentration evolution as function of time in the lower compartment:

$$C_t = C_0 e^{-\frac{D_0 \phi \tau A t}{L V_{\text{lower}}}} \tag{10}$$

where C_0 (mg/L) is the initial concentration in the lower compartment at time zero and C_t (mg/L) is the final concentration in the lower compartment at time t.

Eq. (10) can also be expressed for the temporal concentration evolution of one individual isotopologue, since the diffusion transport process in the diffusion cells acts on isotopologues. By formulating Eq. (10) for two isotopologues and dividing these equations by each other, the temporal evolution of the ratio of two isotopologues in the lower compartment of the diffusion cell can be expressed as follows:

$$\frac{C_{H,t}}{C_{L,t}} = \frac{C_{H,0}}{C_{L,0}} \frac{e^{-\frac{D_{0,H} \phi \tau A t}{L V_{\text{lower}}}}}{e^{-\frac{D_{0,L} \phi \tau A t}{L V_{\text{lower}}}}} = \frac{C_{H,0}}{C_{L,0}} e^{\frac{-\phi \tau A t (D_{0,H} - D_{0,L})}{L V_{\text{lower}}}} \tag{11}$$

where $C_{H,0}$ (mg/L) is the initial concentration of the heavy isotopologue, $C_{L,0}$ (mg/L) is the initial concentration of the light isotopologue, $C_{H,t}$ (mg/L) is the concentration of the heavy isotopologue at time t, $C_{L,t}$ (mg/L) is the concentration of the light isotopologue at time t, $D_{0,H}$ (m^2/s) refers to the diffusion coefficient of the heavy isotopologue in free solution and $D_{0,L}$ (m^2/s) refers to the diffusion coefficient of the light isotopologue in free solution.

Expanding the right term of Eq. (11) by power to $\frac{D_{0,L}}{D_{0,L}}$ and expressing the isotopologue ratios at time t and time zero by R_t and R_0, respectively leads to the following equation:

$$R_t = R_0 e^{\left[\frac{-\phi \tau A t (D_{0,H} - D_{0,L})}{L V_{\text{lower}}}\right]^{\frac{D_{0,L}}{D_{0,L}}}} = R_0 e^{\left(\frac{-\phi \tau A t D_{0,L}}{L V_{\text{lower}}}\right)\left(\frac{D_{0,H}}{D_{0,L}} - 1\right)} \tag{12}$$

Eq. (12) corresponds to a typical Rayleigh type equation of the form $R_t = R_0 f^{(\alpha - 1)}$, where the term $e^{\left(\frac{-\phi \tau A t D_{0,L}}{L V_{\text{lower}}}\right)}$ equals the remaining fraction f of the species in the lower

compartment and $\frac{D_{0,H}}{D_{0,L}}$ corresponds to the fractionation factor α. Therefore Eq. (12) demonstrates that the fractionation between two isotopologues in the lower compartment of the diffusion cell follows a typical Rayleigh type behavior with a constant fractionation factor α and that the magnitude of fractionation depends only on the ratio between the diffusion coefficients in free solution of the two isotopologues. For convenience, Eq. (12) was multiplied by a factor of 1000 and the natural logarithm was taken, which results in the following equation:

$$[\ln(R_t/R_0)] \times 1000 = \left(\frac{D_{0,H}}{D_{0,L}} - 1\right) \times 1000 \ln f \quad (13)$$

Hence, by plotting $[\ln(R_t/R_0)] \times 1000$ vs. $\ln f$, the ratio of the diffusion coefficients in free solution for heavy and light isotopologues can be obtained using linear regression. The usage of isotopologue ratios in Eq. (13) instead of isotope ratios provides the advantage that the determined ratio of $\frac{D_{0,H}}{D_{0,L}}$ in Eq. (13) can be used to evaluate the β values (Eq. (4)) for the corresponding isotopologue pairs. To obtain the uncertainty of diffusion coefficient ratios $\left(\frac{D_{0,H}}{D_{0,L}}\right)$ using the slope of the linear regression in the plotting space $[\ln(R_t/R_0)] \times 1000$ vs. $\ln f$ (Eq. (13)), the 95% confidence interval of the slope of the regression line was calculated according to the following equation:

$$m = \pm t_{0.025,n-2} \times S_m \quad (14)$$

where m is the slope of the regression line, $t_{0.025,n-2}$ is the t-distribution for the 95% confidence interval, n is the degree of freedoms and S_m is the standard deviation of the regression line. The uncertainty of beta values was calculated according to Gauss' error propagation law including the uncertainty of the determined diffusion coefficient ratios.

3. SITE DESCRIPTION

For comparing laboratory with field results, samples were taken from a saturated clay unit, which underlies a chemical waste landfill. The clay consists mainly of Smectite, Illite and Kaolinite and has sandy layers showing a higher permeability than the clay. During the deposition period (~45 years), hazardous waste including organic contaminants was placed on top of the clay and remained in place until remediation of the site. During the period of waste storage, diffusion was expected to be the predominant process for transporting organic contaminants away from the waste landfill into the underlying clay. In April 2013, a clay core of 45 cm length was retrieved from the saturated bottom of the waste landfill and subsampled as a function of depth to analyze concentrations and isotopic evolution with increasing distance from the source for the landfill age of about 45 years.

4. SAMPLING, ANALYTICAL METHODS AND DATA EVALUATION

4.1. VOC extraction from clay core

Volatile organic compounds (VOCs) were extracted from the clay core following the procedure described by Parker (1996): The retrieved clay core (diameter : 20 cm) was split longitudinally in two pieces of the same size. After splitting, the core was logged (photographs and description) for geological features. Logging was performed as fast as possible (~5 min) to prevent any loss of VOCs. Afterwards subsampling was carried out with a spacing of 5 cm to gain a satisfactory resolution of the concentration and isotopic data of the VOCs as a function of depth. Subsamples of about 3 cm length were taken from the clay core using a mini corer (inner diameter: 16 mm, length: 110 mm) and a plunger (diameter: 15 mm, length: 125 mm), both made of stainless steel. To prevent any loss of VOC during subsampling, the clay core was covered by aluminum foil except at the place, where subsampling took place. The subsamples were extruded by the plungers into 42 mL glass vials containing 20 mL high purity (>99.7%) methanol (MeOH). A high clay to MeOH ratio (typically 0.8) was chosen to maximize the amount of VOCs in the MeOH extracts. Subsequently the vials were sealed with a screw cap with a Teflon lined septum. The vials were weighted before and after the collection of the clay samples to determine the weight of the solid samples.

In the laboratory, the 42 mL vials were sonicated for 30 min followed by shaking for 1 h in order to disperse the clay samples and to dissolve all VOC completely in the MeOH. Afterwards, the vials were centrifuged for 30 min at 1200 rpm to obtain a clear MeOH supernatant. The clear MeOH supernatant was then decanted in 4 mL vials, which were sealed with a screw cap with Teflon lined septum for storage prior to analysis.

4.2. VOC concentration analysis

VOC concentrations in water samples were analyzed using a Trace™ GC-DSQII mass spectrometer (Thermo Fisher Scientific, Waltham, MA, US) operated in selected ion mode with a detection limit of 2.0 µg/L. Calibration curves for cDCE, TCE, tetrachloroethene (PCE), 1,1,2,2-tetrachloroethane (TCA) and 1,2-DCA were produced using external standards (purity ⩾ 95.0%), which were prepared at seven different concentration levels: 5, 10, 25, 50, 75, 100, 150 µg/L. Headspace samples from 20 mL vials filled with 10 mL sample were injected using a CombiPal auto sampler (CTC Analytics, Zwingen, Switzerland). Based on an initial screening of VOC concentrations, the samples were diluted to approximately identical concentrations (50 µg/L) to fit the calibration interval and to maximize precision of the analysis. For samples containing cDCE, TCE, PCE and 1,1,2,2-TCA, the GC oven temperature was held at 40 °C for 2 min, ramped at 15 °C/min to 130 °C and held for 2 min. For samples with 1,2-DCA, the oven temperature was held at 40 °C for 2 min, ramped at 15 °C/min to 90 °C and held for 2 min. The carrier gas was helium with a flow rate of 1,2 ml/min. The analytical uncertainty (1σ) of the concentration measurements was determined by a repeated measurement of standards included in the sample sequence (standards/samples = 1/5) and corresponded to ±5% ($n = 10$) for cDCE, TCE, PCE and 1,1,2,2-TCA and of ±4%, ($n = 5$) for 1,2-DCA.

For analyzing VOC concentrations in the clay samples, aliquots of the MeOH extracts were diluted at least 10 times with pure water and analyzed analogously to water samples. The dilution was made because the polar MeOH is incompatible with the non-polar column of the gas chromatograph. The total soil concentrations were calculated according the following formula:

$$C_s = \frac{V_m C_m}{m_{ws}} \tag{15}$$

where C_s (mg/kg) is the VOC concentration in the wet clay, V_m (L) is the total volume of methanol, C_m (mg/L) is the VOC concentration in the methanol and m_{ws} (kg) is the total mass of the wet clay. The detection limit for VOCs concentrations in the wet clay is approximately 0.05 mg/kg for a typical clay to MeOH ratio of 0.8.

4.3. Carbon isotopes

Compound-specific carbon isotope measurements of TCE and 1,2-DCA were performed using a purge-and-trap concentrator (Tekmar Velocity XPT, USA) coupled to a TRACE™ gas chromatograph (GC) and a DeltaPlus XP isotope mass spectrometer (IRMS) via a combustion III interface (Thermo Finnigan, Germany). Water samples were diluted to identical concentrations of 30 μg/L in 42 mL glass vials with PTFE-lined screw cap to maximize precision of the measurements. The MeOH extracts from the field samples were also diluted to identical concentrations of 30 μg/L but the dilution had to be at least 100 times due to the incompatibility of the MeOH with the purge-and-trap concentrator and the column of the GC. Prior analysis, pre-concentration of samples was performed with the purge-and-trap system by purging 25 mL for ten minutes with N_2 (40 ml/min) and trapping the VOCs on a Vocarb 3000 trap. After desorption, the compounds were transferred to a cryogenic trap (Tekmar Dohrmann) in the GC oven set to −80 °C. The trap was heated to 180 °C to release the compounds to the GC column (DB-VRX, 60 m, 0.25 mm, 1,2 μm) for chromatographic separation. The GC oven temperature for TCE analysis was held at 50 °C for 2 min, then ramped at 5 °C/min to 135 °C and held for 2 min. For 1,2-DCA the temperature was held at 60 °C and then ramped at 5 °C/min to 135 °C and held for 2 min. The carrier gas was helium with a constant flow of 1.2 ml/min. Carbon isotope signatures of TCE and 1,2-DCA were analyzed relative to a standard and expressed in the delta notation (VPDB $\delta = (R/R_{\text{std}} - 1) * 1000$ (‰), where R and R_{std} are the isotope ratios of the sample and the standard, respectively. The analytical uncertainty for experimental water samples (standard deviation of the mean: $\text{SDM} = 1\sigma/\sqrt{n}$, σ: standard deviation, n: sample number) of each TCE and 1,2-DCA measurements was determined based on triplicate measurements. In contrast, field samples were analyzed twice due to the limited samples volume. Thus, the standard deviation of the mean (±SDM) of the field samples was determined based on the standard deviation (1σ) of standards included in the samples sequence ($\sigma = 0.30‰$, $n = 15$).

4.4. Chlorine isotopes

Compound-specific chlorine isotope measurement of TCE and 1,2-DCA was performed using a gas chromatograph coupled to a quadrapole mass spectrometer (GC-qMS; Agilent 7890A, Agilent 5975C). Samples were injected by a headspeace method from 20 mL vials filled with 15 mL solution using a CompiPal Autosampler (CTC Analytics, Zwingen, Switzerland). For chromatographic separation a DB-5 column (30 m, 0.25 mm, 0.25 μm, Agilent) with a constant helium flow of 1,2 ml/min was used. Water samples and MeOH extracts were diluted to identical concentrations of 30 μg/L to maximize precision of the measurements. For the MeOH extracts from the field, the dilution had to be at least 10 times due to the incompatibility of the MeOH with the column of the GC. The analytical uncertainty (±SDM) of each TCE and 1,2-DCA measurements was based on a tenfold measurement of each sample from two different vials (5 replicates from each vial).

The TCE samples and standards were diluted to identical concentrations of 100 μg/L to obtain identical peak areas and thus to maximize precision of the measurements. The temperature program of the GC for TCE was started at 35 °C for 2 min and then ramped at 10 °C/min to 50 °C and held for 0.2 min. All four chlorine isotopologues intensities of TCE (mass 130, 132, 134, 136) were quantified using the GC-qMS. Thus raw chlorine isotopic ratios were calculated with the method developed by Sakaguchi-Soder et al. (2007) and further improved by Aeppli et al. (2010), which takes all chlorine isotopologue of TCE (130, 132, 134 and 136) into account. The raw chlorine isotopic ratios of TCE were then calculated using the following equation:

$$R_{\text{TCE}} = \frac{I_{132} + 2I_{134} + 3I_{136}}{3I_{130} + 2I_{132} + I_{134}} \tag{16}$$

where I is the corresponding molecular ion abundance at different m/z values.

A calibration of raw isotope ratio (Eq. (16)) was performed with two external TCE standards having different chlorine isotope ratios (EIL1 = 3.05‰ and EIL2 = −2.70‰). The standards were previously determined by an IRMS after conversion to methyl chloride using the Holt method (Holt et al., 1997) at the University of Waterloo. Calibration with external standards was performed to receive delta values on the SMOC scale. A recent inter laboratory comparison for different GC-qMS equipment, demonstrated that a lack of calibration of raw GC-qMS chlorine isotope ratios potentially leads to variation of the difference in isotope ratios between two samples by as much as a factor of 1.3 (Bernstein et al., 2011).

The 1,2-DCA samples and standards were also diluted to identical concentrations of 2000 μg/L to obtain identical peak areas and thus to maximize precision of the analysis. The temperature program of the GC for 1,2-DCA was held at 40 °C for 1.8 min and then ramped at 25 °C/min to 120 °C and held for 0.2 min. Chlorine isotopic raw ratios of 1,2-DCA were determined from the two most abundant

fragment ion peaks (m/z 64 and 62) in combination with the general equation for the chlorine isotopic ratios for symmetric molecules developed by Elsner and Hunkeler (2008). For 1,2-DCA this equation corresponds to:

$$R_{1,2\text{-DCA}} = \frac{I_{64}}{I_{62}} \quad (17)$$

where I is the corresponding fragment ion abundance of 1,2-DCA at different m/z values.

As for TCE, received raw chlorine isotope ratios from 1,2-DCA fragments (Eq. (17)) were calibrated against two external standards having different chlorine isotopic ratios (CHYN1 = 6.30‰ and CHYN2 = −0.84‰) to obtain delta values on the SMOC scale. The standards were characterized by the Holt method (Holt et al., 1997) at the Helmholtz Centre in Munich.

4.5. Isotope and isotopologue data evaluation

Since fractionation of isotopically distinct species of chlorinated hydrocarbons occurs between isotopologues and not between isotopes, isotope effects associated with diffusion are characterized by considering isotopologue rather than isotope ratios as justified in more detail for carbon and chlorine in the following paragraph.

4.5.1. Carbon isotopes vs. carbon isotopologues

As demonstrated in the Supplementary information, carbon isotope ratios ($^{13}C/^{12}C$), measured in the delta notation, fractionate proportionally to carbon isotopologue pairs differing in one heavy carbon isotope ($^{13}C/^{12}C \propto C_{HL}/C_{LL}$ and C_{HH}/C_{HL}). This proportionality implies no information loss when considering only one of the two proportional isotopologue pairs. Due to the low abundance of the heavy carbon isotope (^{13}C 1.07% vs. ^{12}C 98.93%), in the present study only the most abundant TCE and 1,2-DCA carbon isotopologue pairs containing one and zero heavy carbon isotope, respectively ($^{131}TCE/^{130}TCE$ and $^{101}1,2DCA/^{100}1,2DCA$) are considered, which is coherent with previous studies (Elsner and Hunkeler, 2008; Neumann et al., 2009; Jin et al., 2013).

4.5.2. Chlorine isotopes vs. chlorine isotopologues

In contrast to carbon, both chlorine isotopes are present at high abundance (^{37}Cl 24.22% vs. ^{35}Cl 75.78%) therefore, also several chlorine isotopologues are present at high abundance. As shown theoretically and experimentally by previous studies (Elsner and Hunkeler, 2008; Jeannottat and Hunkeler, 2012), TCE chlorine isotope ratios ($^{37}Cl/^{35}Cl$) behave proportional to TCE isotopologue pairs differing in one heavy chlorine isotope analogously to carbon. The possibility of tracking TCE chlorine isotopologues directly (Eq. (16)) permits verification of this proportionality. This study confirmed that TCE chlorine isotope ratios ($^{37}Cl/^{35}Cl$) are proportional to TCE chlorine isotopologue pairs differing in one heavy chlorine isotope ($^{132}TCE/^{130}TCE$ and $^{134}TCE/^{132}TCE$) (Fig. 2). For 1,2-DCA, chlorine isotope ratios are also expected to fractionate proportionally to isotopologue pairs differing in one heavy chlorine isotope ($^{37}Cl/^{35}Cl \propto {}^{102}1,2DCA/^{100}1,2DCA$ and $^{100}1,2DCA/^{98}1,2DCA$) as demonstrated in the Supplementary information for 1,2-DCA and more generally for symmetric molecules by Elsner and Hunkeler (2008). The proportionality among TCE and 1,2-DCA chlorine isotopologue pairs differing in one heavy chlorine isotope also results in equal beta values (Eqs. (13) and (4)) since the change of mass ratios between isotopologue pairs differing by one heavy chlorine isotope affects the beta value only within the uncertainty. Therefore, the present study considers only the most abundant TCE and 1,2-DCA chlorine isotopologue pairs differing by on heavy chlorine isotope ($^{132}TCE/^{130}TCE$ and for 1,2-DCA $^{102}1,2DCA/^{100}1,2DCA$).

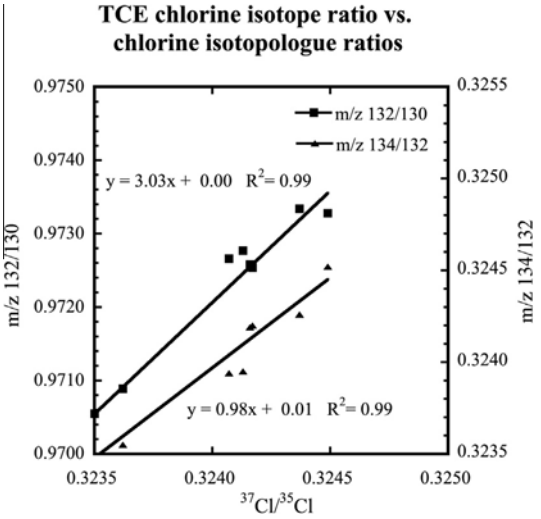

Fig. 2. Relation between TCE chlorine isotope ratio ($^{37}Cl/^{35}Cl$) and TCE chlorine isotopologue pairs differing in one heavy chlorine isotope ($^{132}TCE/^{130}TCE$ and $^{134}TCE/^{132}TCE$). The chlorine isotopologue pairs differing by one heavy chlorine isotope correlate ($R^2 = 0.99$) with the chlorine isotope ratios with a slope of three and one, respectively and intercepting the origin.

5. RESULTS

5.1. Diffusion cell experiment

Initial concentrations of TCE and 1,2-DCA in the lower compartment of the diffusion cell ranged between 22.6 and 901 mg/L (Table 1), while final concentrations after performance of different time series of diffusion cell experiment were between 8.2 and 199 mg/L (Table 1). Initial and final concentrations of each time series of the experiment were used to determine diffusive transport rates acting on TCE and 1,2-DCA in both diffusion cells by calculating effective diffusion coefficients (Eqs. (7) and (10)). Effective diffusion coefficients for TCE and 1,2-DCA in both diffusion cells ranged from 1.28E-10 to 2.20E-10 m^2/s (TCE; Table 1) and from 8.96E-11 to 1.75E-10 m^2/s (1,2-DCA; Table 1), respectively. The effective diffusion coefficients are lower than published diffusion coefficients in free aqueous solutions of TCE (1.01E-9 m^2/s) (Pankow and Cherry, 1996) and 1,2-DCA (9.70E-10 m^2/s) (Gordon, 1999) due to tortuosity and porosity effects affecting the diffusing

Table 1
Effective diffusion coefficients and D_e/D_0 ratios of diffusion cells P2 and P3. Uncertainty of D_e/D_0 (±SDM) was determined by a triplicate measurement of cell P2 and a quintuple measurement of cell P3.

Compound	Initial (mg/L)	Final (mg/L)	Fraction	Time (d)	Effective diffusion coefficient D_e (m^2/s)	D_e/D_0	Diffusion cell	D_e/D_0 average
TCE	22.6	8.2	0.364	0.9	2.20E-10	0.22	P2	
1,2-DCA	96.3	33.2	0.345	11.9	1.75E-10	0.18	P2	
1,2-DCA	211	20.4	0.097	26.9	1.69E-10	0.17	P2	0.19 ± 0.02 (P2)
TCE	84.0	63.1	0.751	4.3	1.28E-10	0.13	P3	
TCE	608	28.8	0.047	42.1	1.41E-10	0.14	P3	
TCE	608	114	0.188	18.2	1.79E-10	0.18	P3	
1,2-DCA	88.4	69.1	0.782	4.0	1.19E-10	0.12	P3	
1,2-DCA	901	199	0.221	32.8	8.96E-11	0.09	P3	0.13 ± 0.02 (P3)

species in the frit. The average tortuosity and porosity effects in the two used diffusion cells were quantified by dividing the determined effective diffusion coefficient by published diffusion coefficients in free solution (Eq. (7)). Different D_e/D_0 ratios were obtained for the two cells with values of 0.19 ± 0.02 ($1\sigma = \pm 0.03$, $n = 3$) for P2 and 0.13 ± 0.02 ($1\sigma = \pm 0.03$, $n = 5$) for P3 (Table 1). Both ratios lie within the range of values obtained in previous studies using the classical Stokes diffusion cell (e.g. 0.10–0.49 in Mills et al. (1968)).

With increasing experimental duration, an accumulation of heavy carbon and chlorine isotopologues of TCE and 1,2-DCA in the lower compartment of the diffusion cells was observed (Figs. 3 and 4). Thus, the light carbon and chlorine isotopologues diffused faster than heavy

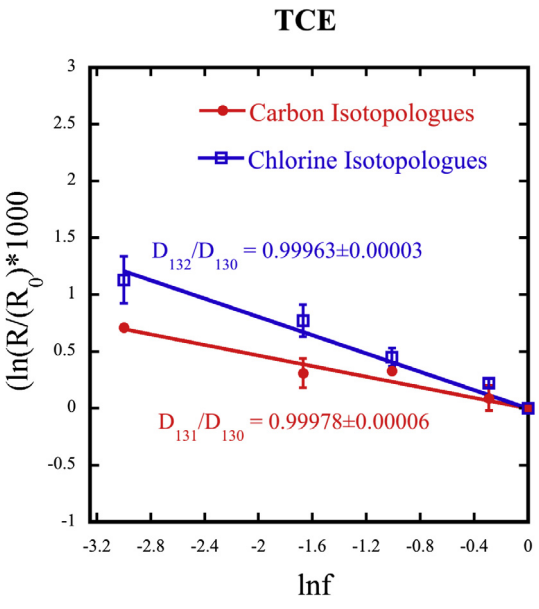

Fig. 3. Rayleigh plot for TCE carbon (red circles) and chlorine (blue squares) isotopologue fractionation in the lower compartment of the diffusion cell. Error bars indicate analytical uncertainty (±SDM) of measurements. Uncertainty of diffusion coefficient ratios of TCE carbon and chlorine isotopologue pairs was calculated based on the 95% confidence interval of the regression line. (For interpretation of the references to color in this figure legend, the reader is referred to the web version of this article.)

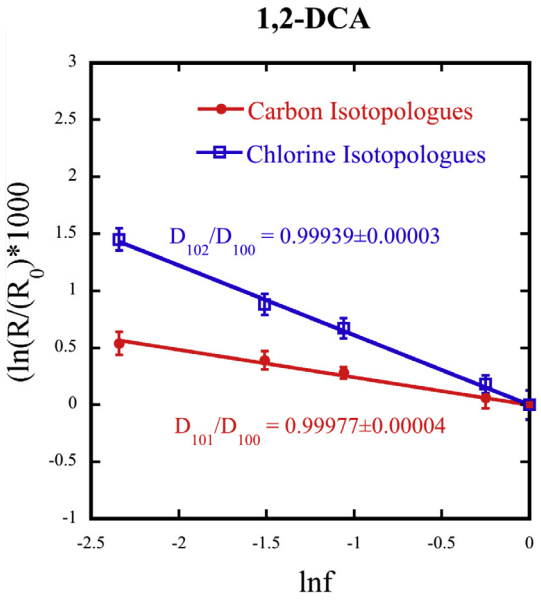

Fig. 4. Rayleigh plot for 1,2-DCA carbon (red circles) and chlorine (blue squares) isotopologue fractionation in the lower compartment of the diffusion cell. Error bars indicate analytical uncertainty (±SDM) of measurements. Uncertainty of diffusion coefficient ratios of 1,2-DCA carbon and chlorine isotopologue pairs was calculated based on the 95% confidence interval of the regression line. (For interpretation of the references to color in this figure legend, the reader is referred to the web version of this article.)

isotopologues through the frit into the upper compartment. The accumulation was stronger for heavy chlorine isotopologues in comparison to heavy carbon isotopologues of TCE and 1,2-DCA. The accumulation of both isotopologue types (carbon and chlorine) followed a Rayleigh trend (Figs. 3 and 4), which is expected given that the Stokes' diffusion cell was modified to a Rayleigh type experiment. The magnitude of isotopologue fractionation was quantified from the slope of the regression line using the Rayleigh equation (Eq. (13)). The diffusion coefficient ratios for TCE isotopologue pairs differing in one heavy isotope gave values of $D_{132}/D_{130} = 0.99963 \pm 0.00003$ for chlorine $D_{131}/D_{130} = 0.99978 \pm 0.00006$ for carbon (Table 1).

For 1,2-DCA, the isotopologue fractionation was stronger for chlorine ($D_{102}/D_{100} = 0.99939 \pm 0.00003$) than

Table 2
Diffusion coefficient ratios and beta values of carbon and chlorine isotopologue pairs of TCE and 1,2-DCA. Uncertainty of diffusion coefficient ratios was calculated based on the 95% confidence interval of regression line (Eqs. (13) and (14)). Uncertainty of beta values was calculated according to Gauss' error propagation law by including the uncertainty of the diffusion coefficient ratios.

Compound	Isotopologue type	D_i/D_j	β in Eq. (4)
TCE	Carbon	$D_{131}/D_{130} = 0.99978 \pm 0.00006$	0.029 ± 0.008
	Chlorine	$D_{132}/D_{130} = 0.99963 \pm 0.00003$	0.024 ± 0.002
1,2-DCA	Carbon	$D_{101}/D_{100} = 0.99977 \pm 0.00004$	0.023 ± 0.004
	Chlorine	$D_{102}/D_{100} = 0.99939 \pm 0.00003$	0.031 ± 0.002

for carbon ($D_{101}/D_{100} = 0.99977 \pm 0.00004$) similarly as for TCE. But when comparing the two compounds, a stronger chlorine isotopologue fractionation was observed for 1,2-DCA relative to TCE, while similar carbon isotopologue fractionation occurred for both compounds (Table 2).

5.2. Diffusion profiles in retrieved core

Four different organic contaminants were found in the clay core from the chemical waste landfill: cDCE, TCE, PCE and 1,1,2,2-TCA (Fig. 5A–D). All four contaminants showed the highest concentration at the top of the clay core reaching values of 2.27 mg/kg (cDCE), 5.69 mg/kg (TCE), 0.11 mg/kg (PCE) and of 0.12 mg/kg (1,1,2,2,-TCA), while with increasing depth the concentrations gradually decreased (Fig. 5A–D). Only concentrations of TCE were high enough to measure isotopologue ratios. Chlorine and carbon isotopologue ratios of TCE displayed a small but significant shift towards smaller values with increasing depth within the clay core (Fig. 6A and B). Carbon isotopologue ratios of TCE (^{131}TCE/^{130}TCE) showed a value of 0.010903 ($\delta^{13}C_{VPDB} = -29.72‰$) at the top of the clay core before the ratio decreased to 0.010898 ($\delta^{13}C_{VPDB} = -30.18‰$) at 40 cm depth ($\Delta\delta^{13}C_{VPDB} = 0.46‰$) (Fig. 6A). The same pattern was observed for the TCE chlorine isotopologue ratios differing in one heavy isotope (^{132}TCE/^{130}TCE): The ratio showed values of 0.97374 ($\delta^{37}Cl_{SMOC} = 1.79‰$) at the top of the clay core decreasing to 0.97324 ($\delta^{37}Cl_{SMOC} = 1.28‰$) at 40cm depth ($\Delta\delta^{37}Cl_{SMOC} = 0.51‰$) (Fig. 6B).

6. DISCUSSION

6.1. Diffusion cell experiment

The observed stronger accumulation of heavy chlorine isotopologues in comparison to heavy carbon isotopologues of TCE and 1,2-DCA is consistent with the mass differences between the stable isotopes of carbon and chlorine. Chlorine isotopologue pairs differ by two mass units in molecular weight, while carbon isotopologue differ only by one. Consequently the fractionation is larger for chlorine than for carbon isotopologues. Furthermore, the larger chlorine isotopologue fractionation for 1,2-DCA compared to TCE (Table 2) is most likely due to the larger relative mass difference caused by an additional heavy chlorine isotope for 1,2-DCA (2.0%) compared to TCE (1.5%). However, a larger fractionation is not observable for the carbon isotopologues pairs of 1,2-DCA in comparison to TCE. Most likely for carbon, the difference is hidden in the uncertainty, given the relatively small mass difference of an additional heavy carbon isotope in comparison to the whole organic molecule (TCE: 0.8% vs. 1,2-DCA: 1%). To evaluate whether chlorine and carbon isotopologue fractionation of TCE and 1,2-DCA shows a similar mass dependence, beta values were calculated (Eq. (4), Table 2). The beta value for the chlorine (0.024 ± 0.002) and carbon (0.029 ± 0.008) isotopologue pairs of TCE agree within the range of uncertainty. The equal beta values indicate that the diffusion coefficient ratios for carbon and chlorine isotopologues of TCE follow the same proportionality on a logarithmic scale with respect to their mass ratios. For 1,2-DCA, the determined beta value for the carbon isotopologue pair (Table 2) agrees within the uncertainty with the value obtained for the TCE carbon isotopologue pair. In contrast, the determined beta value for the 1,2-DCA chlorine isotopologue pair (0.031 ± 0.002) is slightly higher than the value for the carbon isotopologue pair (0.023 ± 0.004). This indicates that the magnitude of carbon and chlorine isotopologue fractionation of 1,2-DCA is not equally proportional on a logarithmic scale in relation to the different mass ratios of the isotopologue pairs. This behavior is not yet fully understood and thus the fractionation of 1,2-DCA chlorine and carbon isotopologues is most likely influenced by other properties in addition to the mass ratios.

Generally, the determined beta values for carbon and chlorine isotopologue pairs of 1,2-DCA and TCE are more than one order of magnitude smaller than 0.5, indicating that the kinetic theory (Eq. (3)) overestimates the magnitude of isotopologue fractionation of 1,2-DCA and TCE during diffusion in the aqueous phase. For the chlorine isotopologues of TCE, Jin et al. (2014) also observed a more than one order of magnitude smaller beta value (0.043) than the value (0.5) postulated by the kinetic theory. Although the beta value obtained by Jin et al. (2014) falls in the same range as the value of the present study (0.024 ± 0.002), the two results differ significantly possibly due to a different analytical approach. In our study, we maximized the accuracy and precision by using a two point calibration, equal concentrations for all samples and standards and 10 repeats for each chlorine sample (cf. chp. 4). The determined beta values of the present study for carbon and chlorine isotopologue pairs of TCE and 1,2-DCA (Table 2) are consistent with recent experimentally determined range of beta values ($0 \leqslant \beta < 0.2$) for diffusing ions in ambient liquid water (Richter et al., 2006), in polyacrylamide gel (Eggenkamp

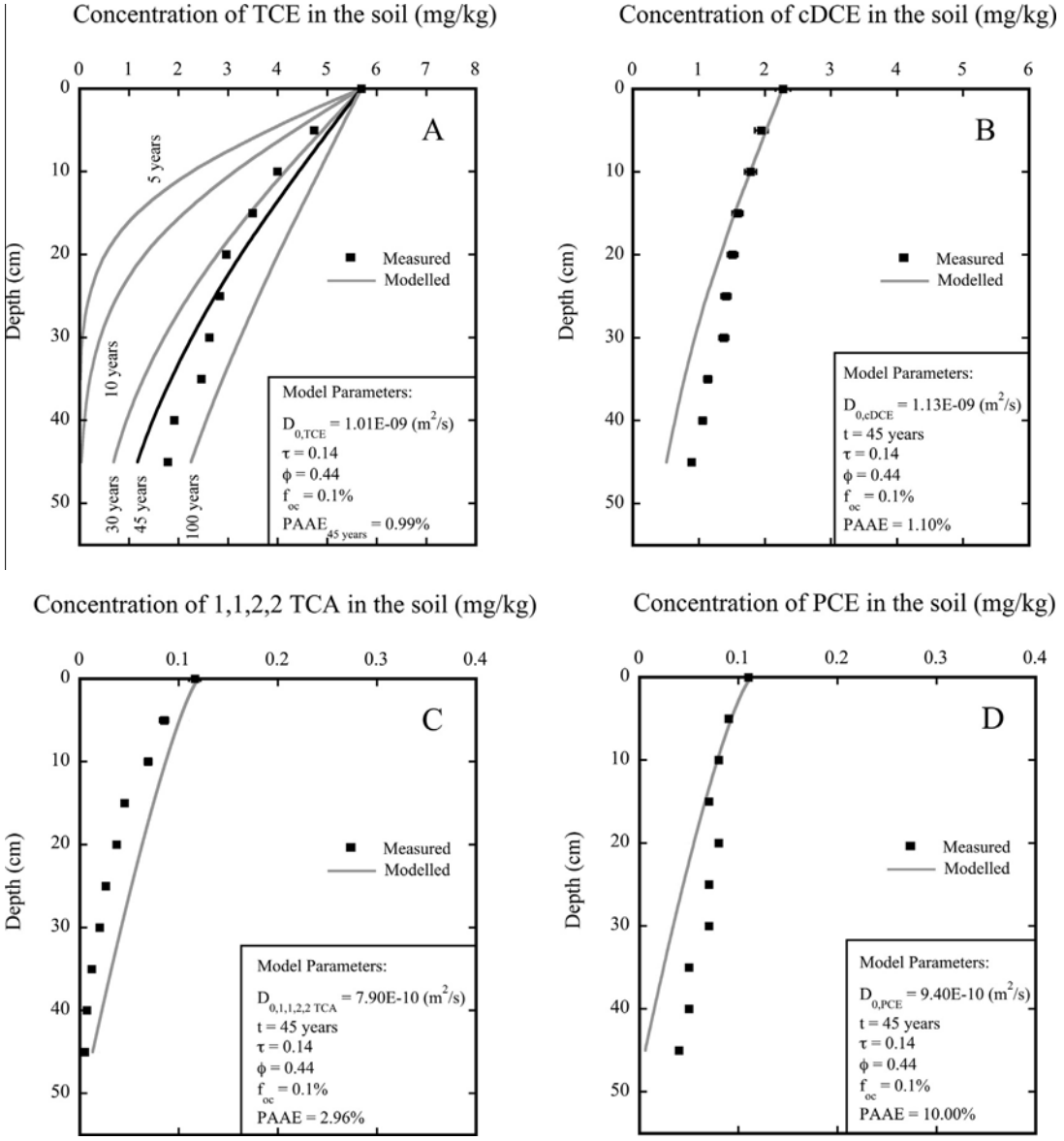

Fig. 5. (A–D) Concentration profiles of TCE (A), cDCE (B), 1,1,2,2-TCA (C) and PCE (D) of the retrieved clay core beneath the chemical waste landfill. Error bars indicate analytical uncertainty ($\pm 1\sigma$). Grey lines indicate simulated concentration evolution in a 1D-diffusion model for a time period of 45 years and additionally in (A) for time periods of 5, 10, 30 and 100 years. A tortuosity factor of 0.14, a clay porosity of 0.44 and a fraction of 0.1% of organic carbon in the clay were used as parameters in the 1D-diffusion model, whereas the tortuosity factor was used as the fitting parameter. A percent average absolute error (PAAE) of 0.99% for TCE (A), of 1.10% for cDCE (B), of 2.96% for 1,1,2,2 TCA (C) and of 10.00% (D) for PCE was determined for quantifying the goodness of the fit between measured and modelled data for the time period of 45 years.

and Coleman, 2009) and in silicate melts (Watkins et al., 2011). Furthermore, obtained beta values are in the same range as values quantified by molecular dynamic simulations for metal ions and noble gases (0.000–0.171) (Bourg and Sposito, 2008; Bourg et al., 2010). Moreover, the determined beta values fall in the same range as observed for carbon isotopologues of methane (0.024–0.055) and ethane (0.021–0.046) (Zhang and Krooss, 2001; Schloemer and Krooss, 2004) and are close to the beta values for deuterated and non-deuterated isotopologues of TBA (0.063) and IPA (0.023) (LaBolle et al., 2008). This confirms the hypothesis, that the kinetic theory (Eq. (3)) overestimates not only the magnitude of isotope fractionation for ions diffusing in water but also for organic compounds. Furthermore, previous kinetic-theory based models of MTBE and TBA transport in a thin high permeability layer bordered by two low permeability zones (LaBolle et al., 2008) likely overestimate the magnitude of isotopologue fractionation due to aqueous phase diffusion.

Moreover, the coherence of the determined beta values with a wide range of other studies also suggests that the experimental determined beta values for perdeuterated

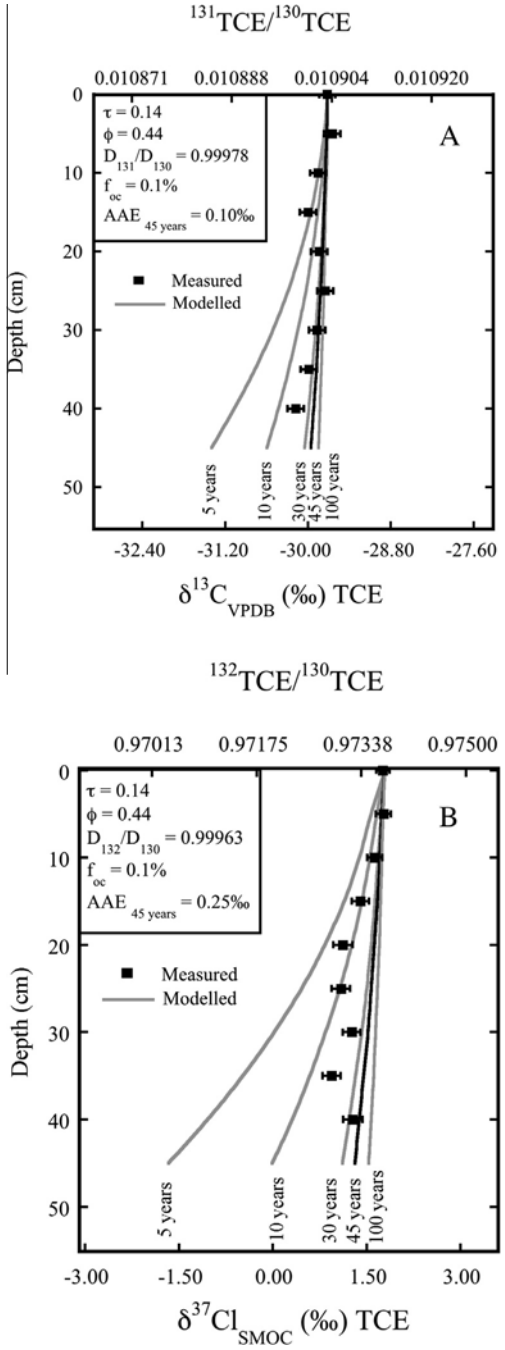

Fig. 6. (A, B) Profiles of TCE carbon (A) and chlorine isotopologues (B) ratios measured in the retrieved clay core beneath the chemical waste landfill. Grey lines indicate simulated isotopic evolution with a 1D-diffusion model for 5, 10, 30, 45 and 100 years. Error bars of TCE carbon and chlorine isotopologue ratio measurements indicate standard error of the mean (±SDM). The same tortuosity factor of 0.14 as for the concentration profile, a clay porosity of 0.44 and an organic carbon fraction of 0.1% in the clay was used in the 1D diffusion model. Diffusion coefficient ratios for TCE carbon ($D_{131}/D_{130} = 0.99978$) and chlorine ($D_{132}/D_{130} = 0.99963$) isotopologue pairs were taken from the diffusion cell experiment. An absolute average error (AAE) of 0.25‰ for chlorine and of 0.10‰ for carbon isotopologue ratios was determined for quantifying the goodness of the fit between measured and modelled ratios for the time period of 45 years.

and non-deuterated isotopologues of toluene and ethylbenzene (0.433) by Jin et al. (2014) are also not representative for molecules with isotope ratios at natural abundance.

6.2. Diffusion profiles in clay core

The concentration profiles of cDCE, TCE, PCE and 1,1,2,2-TCA in the clay core, were fitted using a 1D analytical solution of Fick's second law for a homogeneous, semi-finite porous medium (Crank, 1975; Cussler, 2009) assuming a constant concentration on the top of the clay:

$$C_s(z) = C_{s,0} erfc\left(\frac{z}{2\sqrt{\phi\tau t D_0/R}}\right) \quad (18)$$

where $C_{s,0}$ (mg/kg) is the initial concentration at the top of the clay unit, z refers to the depth (m), $C_s(z)$ (mg/kg) is the concentration at depth z, and R is the retardation factor, which includes the adsorbed mass of the organic contaminants on organic matter in the clay layer. The retardation factor was determined using the well-known relationship:

$$R = 1 + \left(\frac{\rho_b}{\phi}\right) K_d \quad (19)$$

where ρ_b (g/cm^3) is the dry soil bulk density, ϕ (-) is the soil porosity and K_d (ml/g) is the distribution coefficient. The value of K_d was calculated using the well-known relationship $K_d = K_{OC} \times f_{oc}$, where K_{OC} is the soil organic carbon-water portioning coefficient and f_{OC} is the organic matter content in the clay. K_{OC} values of 126 ml/g for TCE, 364 ml/g for PCE, 86 ml/g for cDCE and 118 ml/g for 1,1,2,2-TCA were taken from Pankow and Cherry (1996). Clay porosity (0.44), clay dry bulk density (1.560 g/cm^3), organic matter content in the clay (0.1%), were taken from previous consultant studies. For diffusion coefficients in free solution (D_0), published diffusion coefficients of 9.40E-10 m^2/s for PCE, 1.01E-9 m^2/s for TCE (Pankow and Cherry, 1996),1.13E-9 m^2/s for cDCE and 7.90E-10 m^2/s for 1,1,2,2-TCA (GSI, 2013) were used.

The tortuosity factor (Eq. (18)) was used as the fitting parameter as it is common for such VOC diffusion profiles in clay units (Parker et al., 2004). The goodness of the fit between measured and modeled data was quantified using the percent average absolute error (PAAE). The best fit of the concentration profiles for the landfill age of 45 years was obtained with a tortuosity factor of 0.14 (Fig. 5A–D) with PAAE values $\leqslant$ 10% for all four VOCs. Determined low tortuosity factor is in a plausible range, since Schloemer and Krooss (2004) showed, that in low permeability sediments tortuosity factors are potentially up to three orders of magnitude lower than in free aqueous solutions.

The fact that all four VOC diffusion profiles within the clay core were satisfactorily reproduced with Eq. (18) for the age landfill age of 45 years (PAAE $\leqslant$ 10%) indicates, that diffusion is likely the predominant transport process and that advection and (bio)degradation plays a minor role within the clay core. Furthermore, the advective flow velocity was previously estimated to be less than one mm per year using Darcy's law (unpublished consultant study) confirming that diffusion is the predominant transport

process in the clay layer. Therefore, the small shift of carbon and chlorine isotopologue ratios towards smaller values with increasing depth in the clay unit likely also originates from the diffusive transport. To explore this explanation in more detail, chlorine and carbon isotopologue ratios of TCE were simulated using the experimentally determined diffusion coefficient ratios for TCE carbon and chlorine isotopologue pairs differing in one heavy isotope and the same tortuosity factor (0.14) as for fitting the TCE concentration profile. For this purpose Eq. (18) was expressed for individual isotopologues of TCE and divided by each other:

$$R(z) = \left(\frac{C_H}{C_L}\right)_{\text{Sample}} = \frac{C_{H,0}\,erfc\left(\frac{z}{2\sqrt{\phi\tau t D_{0,H}/R}}\right)}{C_{L,0}\,erfc\left(\frac{z}{2\sqrt{\phi\tau t D_{0,L}/R}}\right)} \quad (20)$$

where $R(z)$ is the evolution of the isotopologue ratio as function of depth in the clay core, $\left(\frac{C_H}{C_L}\right)_{\text{Sample}}$ is the ratio between the heavy and the light isotopologue pair of the sample, $C_{H,0}$ and $C_{L,0}$ are the initial concentrations of the heavy and the light isotopologue at the top of the clay, z (m) is the depth, t (s) is the time, $D_{0,H}$ (m^2/s) and $D_{0,L}$ (m^2/s) are diffusion coefficients in free solution of the heavy and the light isotopologue of TCE, respectively in free solution taken from the diffusion cell experiment ($D_{131}/D_{130} = 0.99978$ and $D_{132}/D_{130} = 0.99963$, cf. chp. 5.1.)

Simulated carbon and chlorine isotopologue profiles for the landfill age of 45 years, fitted well with measured carbon and chlorine isotopologue ratio profiles showing absolute average errors of 0.10‰ for carbon and of 0.25‰ for chlorine isotopologues, which are in the range of the measurement uncertainty (Fig. 6A and B). This indicates, that the magnitude of isotopologue fractionation observed in the clay unit of the field site is consistent with laboratory determined ratios of diffusion coefficients especially for the carbon isotopologue pairs of TCE (Fig. 6A and B). This also suggests that sorption likely has a relatively small influence on isotopologue fractionation, which is consistent with previous findings (Harrington et al., 1999; Slater et al., 2000). Furthermore, simulations for different diffusion periods in the clay unit (5, 10, 30, 45 and 100 years) show how TCE concentrations and carbon and chlorine isotopologue ratio profiles evolve over time in diffusion dominated systems. In the initial stage (5 years), when the concentration gradient is steep (Fig. 5A), a much larger isotopologue effect is observed than in later times (Fig. 6A and B). The difference between the ratios at the top of the clay core and the value at 45 cm depth is almost 0.00275 ($\Delta\delta^{37}Cl_{SMOC} = 2.83‰$) for chlorine isotopologues and 0.000015 ($\Delta\delta^{13}C_{VPDB} = 1.35‰$) for carbon isotopologues. In contrast with increasing time, when the TCE concentration gradient becomes more flat (Fig. 5A), the heavier isotopologues catch up and the isotopologue shift towards lighter isotopologue signatures with increasing depth becomes smaller and almost disappears during long diffusion periods (100 years, Fig. 6A and B). Therefore, although there is a significant isotopologue fractionation during the diffusive transport process, during long diffusion periods, shifts in isotopologue ratios almost completely disappear.

7. CONCLUSIONS AND IMPLICATIONS FOR ENVIRONMENTAL STUDIES

The results of the present study demonstrate that the kinetic theory (Eq. (3)) overestimates the magnitude of carbon and chlorine isotopologue fractionation of TCE and 1,2-DCA during diffusion in the aqueous phase. This outcome is consistent with experimentally determined beta values for the fractionation of diffusing ions (Richter et al., 2006; Eggenkamp and Coleman, 2009), noble gases (Tempest and Emerson, 2013; Tyroller et al., 2014) and different isotopologue types of organic compounds (Zhang and Krooss, 2001; Schloemer and Krooss, 2004; LaBolle et al., 2008; Jin et al., 2014). Furthermore, the results of the present study are consistent with molecular dynamic simulations addressing metal cations and noble gases (Bourg and Sposito, 2008; Bourg et al. 2010). Thus, our results confirm that the kinetic theory not only fails for the prediction of isotope fractionation of diffusing ions and noble gases in the aqueous phase, but also for organic compounds. Furthermore, by including the laboratory determined diffusion coefficient ratios in a 1D-diffusion model, the present study relates for the first time consistently laboratory with field values for chlorinated hydrocarbons. Thus, the measurements and simulations demonstrate that the kinetic theory is also not suitable for assessing isotopologue fractionation in diffusion dominated low permeable systems at the field scale. Therefore, previous kinetic theory based modeling studies have overestimated isotope effects during diffusive transport of organic compounds in saturated systems (LaBolle et al., 2008; Rolle et al., 2010; Van Breukelen and Rolle, 2012). Furthermore, simulations for different time periods showed that large shifts in isotopologue ratios will only occur during short diffusion periods. Consequently, diffusion-caused isotopologue fractionation in water-saturated low permeability sediment only impairs the identification of reactive processes using CSIA during short diffusion periods, when diffusion-rated shifts in isotopologue ratios are largest and shifts related to reactive processes might still be small. The diffusion coefficient ratios for carbon and chlorine isotopologues of TCE and 1,2-DCA from this study can help to improve models that incorporate isotope data to identify reactive processes.

ACKNOWLEDGMENTS

The authors acknowledge the Swiss National Science Foundation (SNSF) for their financial support. Furthermore, the authors thank Prof. Ian Bourg and two anonymous reviewers for their constructive comments, which greatly helped to improve the quality of the manuscript.

APPENDIX A. SUPPLEMENTARY DATA

Supplementary data associated with this article can be found, in the online version, at http://dx.doi.org/10.1016/j.gca.2015.02.034.

REFERENCES

Aeppli C., Holmstrand H., Andersson P. and Gustafsson O. (2010) Direct compound-specific stable chlorine isotope analysis of organic compounds with quadrupole GC/MS using standard isotope bracketing. *Anal. Chem.* **82**, 420–426.

Alder B. J., Alley W. E. and Dymond J. H. (1974) Studies in molecular-dynamics. 14. Mass and size dependence of binary diffusion coefficients. *J. Chem. Phys.* **61**, 1415–1420.

Appelo C. A. J. and Postma D. (2005). .

Asfour A. F. A. (1983) Improved and simplified diaphragm cell design and analysis technique for calibration. *Rev. Sci. Instrum.* **54**, 1394–1396.

Asfour A. F. A. and Dullien F. A. L. (1983) Diaphragm diffusion cell – simpler cell design and new equation to calculate diffusivities. *AIChE J.* **29**, 347–349.

Ballentine C. J., Burgess R. and Marty B. (2002) Tracing fluid origin, transport and interaction in the crust. In *Noble Gases in Geochemistry and Cosmochemistry* (eds. D. Porcelli, C. J. Ballentine and R. Wieler). Mineralogical Society of America. pp. 539–614.

Bear J. (1972) *Dynamics of Fluids in Porous Media*. Dover, New York.

Beekmann H. E., Eggenkamp H. G. M. and Appelo C. A. J. (2011) An integrated modelling approach to reconstruct complex solute transport mechanism – Cl and δ^{37}Cl in pore water of sediments from a former brackish lagoon in The Netherlands. *Appl. Geochem.* **26**, 257–268.

Berkowitz M. and Wan W. (1987) The limiting ionic conductivity of Na^+ and CL^- ions in aqueous solutions – molecular dynamics simulation. *J. Chem. Phys.* **86**, 376–382.

Bernstein A., Shouakar-Stash O., Ebert K., Laskov C., Hunkeler D., Jeannottat S., Sakaguchi-Soder K., Laaks J., Jochmann M. A., Cretnik S., Jager J., Haderlein S. B., Schmidt T. C., Aravena R. and Elsner M. (2011) Compound-specific chlorine isotope analysis: a comparison of gas chromatography/isotope ratio mass spectrometry and gas chromatography/quadrupole mass spectrometry methods in an interlaboratory study. *Anal. Chem.* **83**, 7624–7634.

Biswas R. and Bagchi B. (1997) Limiting ionic conductance of symmetrical, rigid ions in aqueous solutions: temperature dependence and solvent isotope effects. *J. Am. Chem. Soc.* **119**, 5946–5953.

Bouchard D., Hohener P. and Hunkeler D. (2008a) Carbon isotope fractionation during volatilization of petroleum hydrocarbons and diffusion across a porous medium: a column experiment. *Environ. Sci. Technol.* **42**, 7801–7806.

Bouchard D., Hunkeler D., Gaganis P., Aravena R., Hohener P., Broholm M. M. and Kjeldsen P. (2008b) Carbon isotope fractionation during diffusion and biodegradation of petroleum hydrocarbons in the unsaturated zone: field experiment at Vaerlose airbase, Denmark, and modeling. *Environ. Sci. Technol.* **42**, 596–601.

Bourg I. C. and Sposito G. (2007) Molecular dynamics simulations of kinetic isotope fractionation during the diffusion of ionic species in liquid water. *Geochim. Cosmochim. Acta* **71**, 5583–5589.

Bourg I. C. and Sposito G. (2008) Isotopic fractionation of noble gases by diffusion in liquid water: molecular dynamics simulations and hydrologic applications. *Geochim. Cosmochim. Acta* **72**, 2237–2247.

Bourg I. C., Richter F. M., Christensen J. N. and Sposito G. (2010) Isotopic mass dependence of metal cation diffusion coefficient in liquid water. *Geochim. Cosmochim. Acta* **74**, 2249–2256.

Chernyavsky B. M. and Wortmann U. G. (2007) REMAP: a reaction transport model for isotope ratio calculations in porous media. *Geochem. Geophys. Geosyst.* **8**, Q02009.

Chong S. H. and Hirata F. (1998) Dynamics of solvated ion in polar liquids: an interaction-site-model description. *J. Chem. Phys.* **108**, 7339–7349.

Clark I. D. and Fritz P. (1997) *Environmental Isotopes in Hydrogeology*. CRC Press, New York.

Cotel S., Schafer G., Barthes V. and Baussan P. (2011) Effect of density-driven advection on trichloroethylene vapor diffusion in a porous medium. *VZJ* **10**, 565–581.

Crank J. (1975) *The Mathematics of Diffusion*. Oxford University Press, New York.

Cussler E. L. (2009) *Diffusion Mass transfer in Fluid Systems*. Cambridge University Press, New York.

Damgaard I., Bjerg P. L., Baelum J., Scheutz C., Hunkeler D., Jacobsen C. S., Tuxen N. and Broholm M. M. (2013) Identification of chlorinated solvents degradation zones in clay till by high resolution chemical, microbial and compound specific isotope analysis. *J. Contam. Hydrol.* **146**, 37–50.

Desaulniers D. E., Kaufmann R. S., Cherry J. A. and Bentley H. W. (1985) ^{37}Cl–^{35}Cl variations in a diffusion-controlled groundwater system. *Geochim. Cosmochim. Acta* **50**, 1757–1764.

Donahue M. A., Werne J. P., Meile C. and Lyons T. W. (2008) Modeling sulfur isotope fractionation and differential diffusion during sulfate reduction in sediments of the Cariaco Basin. *Geochim. Cosmochim. Acta* **72**, 2287–2297.

Eggenkamp H. G. M. and Coleman M. L. (2009) The effect of aqueous diffusion on the fractionation of chlorine and bromine stable isotopes. *Geochim. Cosmochim. Acta* **73**, 3539–3548.

Elsner M. and Hunkeler D. (2008) Evaluating chlorine isotope effects from isotope ratios and mass spectra of polychlorinated molecules. *Anal. Chem.* **80**, 4731–4740.

Elsner M., Zwank L., Hunkeler D. and Schwarzenbach R. P. (2005) A new concept linking observable stable isotope fractionation to transformation pathways of organic pollutants. *Environ. Sci. Technol.* **39**, 6896–6916.

Falta R. W. (2005) Dissolved chemical discharge from fractured clay aquitards contaminated by DNAPLs. In *Amer Geophysical Union* (eds. B. Faybishenko, P. A. Witherspoon and J. Gale). Dynamics of Fluids and Transport in Fractured Rock, pp. 165–174.

Feenstra S., Mackay D. M. and Cherry J. A. (1991) A method for assessing residual NAPL based on organic-chemical concentrations in soil samples. *Ground Water Monit. R.* **11**, 128–136.

Gordon S. L. (1999) A laboratory method for investigations of diffusion and transformation of volatile organic compounds in low permeability media. Ph. D. thesis, Waterloo Univ.

GSI (2013) GSI Environmental Inc., Chemical Properties Database, Houston.

Harrington R. R., Poulson S. R., Drever J. I., Colber P. J. S. and Kelly E. F. (1999) Carbon isotope systematics of monoaromatic hydrocarbons: vaporization and adsorption experiments. *Org. Geochem.* **30**, 765–775.

Holt B. D., Sturchio N. C., Abrajano T. A. and Heraty L. J. (1997) Conversion of chlorinated volatile organic compounds to carbon dioxide and methyl chloride for isotopic analysis of carbon and chlorine. *Anal. Chem.* **69**, 2727–2733.

Huang L., Sturchio N. C., Abrajano T., Heraty L. J. and Holt B. D. (1999) Carbon and chlorine isotope fractionation of chlorinated aliphatic hydrocarbons by evaporation. *Org. Geochem.* **30**, 777–785.

Hunkeler D., Aravena R. and Butler B. J. (1999) Monitoring microbial dechlorination of tetrachloroethene (PCE) in groundwater using compound-specific stable carbon isotope ratios:

microcosm and field studies. *Environ. Sci. Technol.* **33**, 2733–2738.

Hunkeler D., Aravena R., Berry-Spark K. and Cox E. (2005) Assessment of degradation pathways in an aquifer with mixed chlorinated hydrocarbon contamination using stable isotope analysis. *Environ. Sci. Technol.* **39**, 5975–5981.

Hunkeler D., Abe Y., Broholm M. M., Jeannottat S., Westergaard C., Jacobsen C. S., Aravena R. and Bjerg P. L. (2011) Assessing chlorinated ethene degradation in a large scale contaminant plume by dual carbon-chlorine isotope analysis and quantitative PCR. *J. Contam. Hydrol.* **119**, 69–79.

Jeannottat S. and Hunkeler D. (2012) Chlorine and carbon isotopes fractionation during volatilization and diffusive transport of trichloroethene in the unsaturated zone. *Environ. Sci. Technol.* **46**, 3169–3176.

Jeannottat S. and Hunkeler D. (2013) Can soil gas VOCs be related to groundwater plumes based on their isotope signature? *Environ. Sci. Technol.* **47**, 12115–12122.

Jin B., Haderlein S. B. and Rolle M. (2013) Integrated carbon and chlorine isotope modeling: applications to chlorinated aliphatic hydrocarbons dechlorination. *Environ. Sci. Technol.* **47**, 1443–1451.

Jin B., Rolle M., Li T. and Haderlein S. B. (2014) Diffusive fractionation of BTEX and chlorinated ethenes in aqueous solution: quantification of spatial isotope gradients. *Environ. Sci. Technol.* **48**, 6141–6150.

Johnson R. L. and Pankow J. F. (1992) Dissolution of dense chlorinated solvents into groundwater. 2. Source functions for pools of solvent. *Environ. Sci. Technol.* **26**, 896–901.

Klump S., Tomonaga Y., Kienzler P., Kinzelbach W., Baumann T., Imboden D. M. and Kipfer R. (2007) Field experiments yield new insights into gas exchange and excess air formation in natural porous media. *Geochim. Cosmochim. Acta* **71**, 1385–1397.

Kuder T., Philp P. and Allen J. (2009) Effects of volatilization on carbon and hydrogen isotope ratios of MTBE. *Environ. Sci. Technol.* **43**, 1763–1768.

LaBolle E. M., Fogg G. E., Eweis J. B., Gravner J. and Leaist D. G. (2008) Isotopic fractionation by diffusion in groundwater. *Water Resour. Res.* **44**, W07405.

Lavastre V., Jendrzejewski N., Agrinier P., Javoy M. and Evrard M. (2005) Chlorine transfer out of a very low permeability clay sequence (Paris Basin, France): ^{37}Cl and ^{35}Cl evidence. *Geochim. Cosmochim. Acta* **69**, 4949–4961.

Lippmann J., Stute M., Torgersen T., Moser D. P., Hal J. A., Lin L., Borcsik M., Bellamy R. E. S. and Onstott T. C. (2003) Dating ultra-deep mine waters with noble gases and Cl-36, Witwatersrand Basin, South Africa. *Geochim. Cosmochim. Acta* **67**, 4597–4619.

Lo H. Y. (1974) Diffusion coefficients in binary-liquid alkane systems. *J. Chem. Eng. Data* **19**, 236–241.

Lollar B. S., Slater G. F., Slee B., Witt M., Klecka G. M., Harkness M. and Spivack J. (2001) Stable carbon isotope evidence for intrinsic bioremediation of tetrachloroethene and trichloroethene at area 6, Dover Air Force Base. *Environ. Sci. Technol.* **35**, 261–269.

McManus J., Nägler T. F., Siebert C., Wheat C. G. and Hammond D. E. (2002) Oceanic molybdenum isotope fractionation: diagenesis and hydrothermal ridge-flank alteration. *Geochem. Geophys. Geosyst.* **3**, 1–9.

Meckenstock R. U., Morasch B., Griebler C. and Richnow H. H. (2004) Stable isotope fractionation analysis as a tool to monitor biodegradation in contaminated acquifers. *J. Contam. Hydrol.* **75**, 215–255.

Mills R., Woolf L. A. and Watts R. O. (1968) Simplified procedures for diaphragm – cell diffusion studies. *AIChE J.* **14**, 671–673.

Neumann A., Hofstetter T. B., Skarpeli-Liati M. and Schwarzenbach R. P. (2009) Reduction of polychlorinated ethanes and carbon tetrachloride by structural Fe(II) in smectites. *Environ. Sci. Technol.* **43**, 4082–4089.

Nuevo M. J., Morales J. J. and Heyes D. M. (1995) Mass dependence of isotope self-diffusion by molecular-dynamics. *Phys. Rev.* **51**, 2026–2032.

Pankow J. F. and Cherry J. A. (1996) *Dense Chlorinated Solvents and Other DNAPLs in Groundwater*. Waterloo Press, Portland.

Parker B. L. (1996) Effect of molecular diffusion on the persistence of dense immiscible phase organic liquids in fractured porous geologic media. Ph. D. thesis, Waterloo Univ.

Parker B. L., Cherry J. A. and Chapman S. W. (2004) Field study of TCE diffusion profiles below DNAPL to assess aquitard integrity. *J. Contam. Hydrol.* **74**, 197–230.

Peeters F., Beyerle U., Aeschbach-Hertig W., Holocher J., Brennwald M. S. and Kipfer R. (2003) Improving noble gas based paleoclimate reconstruction and groundwater dating using Ne-20/Ne-22 ratios. *Geochim. Cosmochim. Acta* **67**, 587–600.

Poulson S. R. and Drever J. I. (1999) Stable isotope (C, Cl, and H) fractionation during vaporization of trichloroethylene. *Environ. Sci. Technol.* **33**, 3689–3694.

Richter F. M., Mendybaev R. A., Christensen J. N., Hutcheon I. D., Williams R. W., Sturchio N. C. and Beloso, Jr., A. D. (2006) Kinetic isotopic fractionation during diffusion of ionic species in water. *Geochim. Cosmochim. Acta* **70**, 277–289.

Rolle M., Chiogna G., Bauer R., Griebler C. and Grathwohl P. (2010) Isotopic fractionation by transverse dispersion: flow-through microcosms and reactive transport modeling study. *Environ. Sci. Technol.* **44**, 6167–6173.

Sakaguchi-Soder K., Jager J., Grund H., Matthaus F. and Schuth C. (2007) Monitoring and evaluation of dechlorination processes using compound-specific chlorine isotope analysis. *Rapid Comm. Mass Spectrom.* **21**, 3077–3084.

Schloemer S. and Krooss B. M. (2004) Molecular transport of methane, ethane and nitrogen and the influence of diffusion on the chemical and isotopic composition of natural gas accumulations. *Geofuid* **4**, 81–108.

Senftle F. E. and Bracken J. T. (1954) Theoretical effects of diffusion on isotopic abundance ratios in rocks and associated fluids. *Geochim. Cosmochim. Acta* **7**, 61–76.

Seyedabbasi M. A., Newell C. J., Adamso D. T. and Sale T. C. (2012) Relative contribution of DNAPL dissolution and matrix diffusion to the long-term persistence of chlorinated solvent source zones. *J. Contam. Hydrol.* **134**, 69–81.

Shin W. J. and Lee K. S. (2010) Carbon isotope fractionation of benzene and toluene by progressive evaporation. *Rapid Comm. Mass Spectrom.* **24**, 1636–1640.

Slater G. F., Ahad J. M. E., Lollar B. S., Allen-King R. and Sleep B. (2000) Carbon isotope effects resulting from equilibrium sorption of dissolved VOCs. *Anal. Chem.* **72**, 5669–5672.

Steefel C. I. and Maher K. (2009) Fluid-rock interaction: a reactive transport approach. In *Thermodynamics and Kinetics of Water-Rock Interaction* (eds. E. H. Oelkers and J. Schott). Mineralogical Society of America, pp. 485–532.

Stokes R. H. (1950) An improved diaphragm-cell for diffusion studies, and some test of the method. *J. Am. Chem. Soc.* **72**, 763–767.

Strassmann K. M., Brennwald M. S., Peeters F. and Kipfer R. (2005) Dissolved noble gases in the porewater of lacustrine sediments as palaeolimnological proxies. *Geochim. Cosmochim. Acta* **69**, 1665–1674.

Tempest K. and Emerson S. (2013) Kinetic isotope fractionation of argon and neon in during air–water transfer. *Marin. Chem.* **153**, 39–47.

Tyroller L., Brennwald M. S., Mächler L., Livingston D. M. and Kipfer R. (2014) Fractionation of Ne and Ar isotopes by molecular diffusion in water. *Geochim. Cosmochim. Acta* **126**, 60–66.

Van Breukelen B. M. and Rolle M. (2012) Transverse hydrodynamic dispersion effects on isotope signals in groundwater chlorinated solvents' plumes. *Environ. Sci. Technol.* **46**, 7700–7708.

Vangeet A. L. and Adamson A. W. (1964) Diffusion in liquid hydrocarbon mixtures. *J. Phys. Chem.* **68**, 238–246.

Watkins J. M., DePaolo D. J., Ryerson F. J. and Peterson T. P. (2011) Influence of liquid structure on diffusive isotope separation in molten silicates and aqueous solutions. *Geochim. Cosmochim. Acta* **75**, 3103–3118.

Wedlake G. D. and Dullie F. A. L. (1974) Interdiffusion and density-measurements in some binary-liquid mixtures. *J. Chem. Eng. Data* **19**, 229–236.

Zhang T. W. and Krooss B. M. (2001) Experimental investigation on the carbon isotope fractionation of methane during gas migration by diffusion through sedimentary rocks at elevated temperature and pressure. *Geochim. Cosmochim. Acta* **65**, 2723–2742.

Zhou Z., Ballentine C. J., Kipfer R., Schoell M. and Thibodeaux S. (2005) Noble gas tracing of groundwater/coalbed methane interaction in the San Juan Basin, USA. *Geochim. Cosmochim. Acta* **69**, 5413–5428.

Associate editor: Orit Sivan